Korean J. Chem. Eng., 35(2), 337-347 (2018)
DOI: 10.1007/s11814-017-0284-x

pISSN: 0256-1115
eISSN: 1975-7220

Intensification of the processes of dehydrogenation and dewaxing of middle distillate fractions by redistribution of hydrogen between the units

Evgeniya Frantsina†, Nataliya Belinskaya, and Emiliya Ivanchina

National Research Tomsk Polytechnic University, Lenina Avenue, 30, 634050, Tomsk, Russia
(*Received 14 July 2017 • accepted 7 October 2017*)

Abstract−The dehydrogenation and dewaxing of hydrocarbons of middle-distillate fractions, which proceed in the hydrogen medium, are of great importance in the petrochemical and oil refining industries. They increase oil refining depth and allow producing gasoline, kerosene, and diesel fractions used in the production of hydrocarbon fuels, polymer materials, synthetic detergents, rubbers, etc. Herewith, in the process of dehydrogenation of hydrocarbons of middle distillate fractions (C_9-C_{14}) hydrogen is formed in the reactions between hydrocarbons, and the excess of hydrogen slows the target reaction of olefin formation and causes the shift of thermodynamic equilibrium to the initial substances. Meanwhile, in the process of hydrodewaxing of hydrocarbons of middle distillate fractions (C_5-C_{27}), conversely, hydrogen is a required reagent in the target reaction of hydrocracking of long-chain paraffins, which ensures required feedstock conversion for production of low-freezing diesel fuels. Therefore, in this study we suggest the approach of intensification of the processes of dehydrogenation and dewaxing of middle distillate fractions by means of redistribution of hydrogen between the two units on the base of the influence of hydrogen on the hydrocarbon transformations using mathematical models. In this study we found that with increasing the temperature from 470 °C to 490 °C and decreasing the hydrogen/feedstock molar ratio in the range of 8.5/1.0 to 6.0/1.0 in the dehydrogenation reactor, the production of olefins increased by 1.45-1.55%wt, which makes it possible to reduce hydrogen consumption by 25,000 Nm^3/h. Involvement of this additionally available hydrogen in the amount from 10,000 to 50,000 Nm^3/h in the dewaxing reactor allows increasing the depth of hydrocracking of long-chain paraffins of middle distillate fractions, and, consequently improving low-temperature properties of produced diesel fraction. In such a way cloud temperature and freezing temperature of produced diesel fraction decrease by 1-4 °C and 10-25 °C (at the temperature of 300 °C and 340 °C respectively). However, when the molar ratio hydrogen/hydrocarbons decreases from 8.5/1.0 to 6.0/1.0 the yield of side products in the dehydrogenation reactor increases: the yield of diolefins increases by 0.1-0.15%wt, the yield of coke increases by 0.07-0.18%wt depending on the feedstock composition, which is due to decrease in the content of hydrogen, which hydrogenates intermediate products of condensation (the coke of amorphous structure). This effect can be compensated by additional water supply in the dehydrogenation reactor, which oxidizes the intermediate products of condensation, preventing catalyst deactivation by coke. The calculations with the use of the model showed that at the supply of water by increasing portions simultaneously with temperature rise, the content of coke on the catalyst by the end of the production cycle comprises 1.25-1.56%wt depending on the feedstock composition, which is by 0.3-0.6%wt lower that in the regime without water supply.

Keywords: Oil Refining, Hydrogen, Dehydrogenation, Hydrodewaxing, Modelling, Middle Distillate

INTRODUCTION

Due to the limited reserves of readily recoverable resources in the modern world, oil production has shifted towards bitumen and heavy oils production [1-3], which necessitates the development of deep oil refining processes, such as hydrotreating, hydroskimming, dehydrogenation, hydrogenation, dewaxing, catalytic cracking, and hydrocracking, as well as the methods to increase their resource efficiency [4-6]. The main products of these processes are gasoline, kerosene, and diesel fractions, which are used in the production of hydrocarbon fuels, polymeric materials, synthetic detergents, rubbers, etc. [7,8]. Due to the active development of the Arctic regions, there has recently been a steady increase in the demand for diesel and jet fuels capable of operating at low temperatures up to −50 °C, which can only be obtained by means of hydrogenation processes [9-11]. Hydrogen plays a special role in these processes, as that particular component is the main reagent in hydrocracking and hydrogenation reactions of long chain paraffins and aromatic hydrocarbons, leading to the formation of low molecular weight paraffins with improved low-temperature properties [12,13]. Hydrogen is an important feedstock component of both the chemical and oil industries and is considered to be the energy carrier of the future [14,15].

Hydrogen is an expensive component, and the processes of its production are complicated and time-consuming due to their non-stationary nature, caused by change in feedstock composition, catalyst activity and technological conditions of the processes [16-18]. For these reasons, the tasks related to developing models of such

†To whom correspondence should be addressed.
E-mail: evf@tpu.ru

processes, which allow forecasting of the yield and quality of the product depending on the feedstock composition, catalyst activity and technological conditions of the process, are of particular relevance [19-21]. These models are developed on the base of physical-chemical regularities of hydrocarbon transformations on the catalyst surface [22-26].

The aim of our work was to suggest the way of intensification of the processes of dehydrogenation and dewaxing of middle distillate fractions by means of redistribution of hydrogen between the two units on the base of the influence of hydrogen on the hydrocarbon transformations using mathematical models.

OBJECT OF RESEARCH

1. Apparatus and Catalysts

Reactors with a circulation loop of hydrogen for catalytic refining of the middle distillate fractions in the processes of paraffin dehydrogenation (C_9-C_{14}) and hydrocarbon dewaxing (C_5-C_{27}) were used as the research objects. These reactors are industrial apparatuses used for catalytic processes of dehydrogenation and dewaxing.

The reactor for dehydrogenation of paraffins of middle distillate fractions (C_9-C_{14}) is a vessel with a radial feedstock entering, in which a fixed bed of Pt-catalyst is loaded. The dehydrogenation process is carried out in the hydrogen medium at the following technological conditions: temperature of 470-490 °C, pressure of 0.2 MPa, and hydrogen/feedstock molar ratio of 8.5/1.0-6.0/1.0 (Fig. 1) [27,28]. The feedstock is introduced into the reactor from the top, then passes through the fixed bed of granular catalyst consisting of Al_2O_3 or aluminosilicate impregnated with platinum. The catalyst service life can be from 200 to 400 days. The product mixture goes out from the reactor through a perforated pipe located around the vertical axis of the reactor. The main purpose of the process is to obtain normal olefins by dehydrogenating the paraffins of kerosene fraction (C_9-C_{14}) in the production of synthetic detergents [29,30]. The process conversion is 8-10% with selectivity in terms of olefins equal to 90%.

The reactor for dewaxing of paraffins of middle distillate fractions (C_5-C_{27}) is a vertical vessel of axial type with a fixed bed of Ni-catalyst. The dewaxing process is carried out in a hydrogen medium under the following technological conditions: the temperature of 330-360 °C, the pressure of 7.0 MPa, the hydrogen flow rate of 50,000 Nm^3/h (Fig. 2). The feedstock sequentially passes through three layers of dewaxing Ni-catalyst and the layer of hydrotreating Co-Mo-catalyst. The latter is intended to remove unsaturated compounds and mercaptans that are produced during the dewaxing process. To provide separation between the layers of the dewaxing Ni-catalyst and hydrotreating Co-Mo-catalyst, a layer of inert balls is loaded between them, as well as at the bottom of the reactor. The height of the reactor is much higher than its diameter

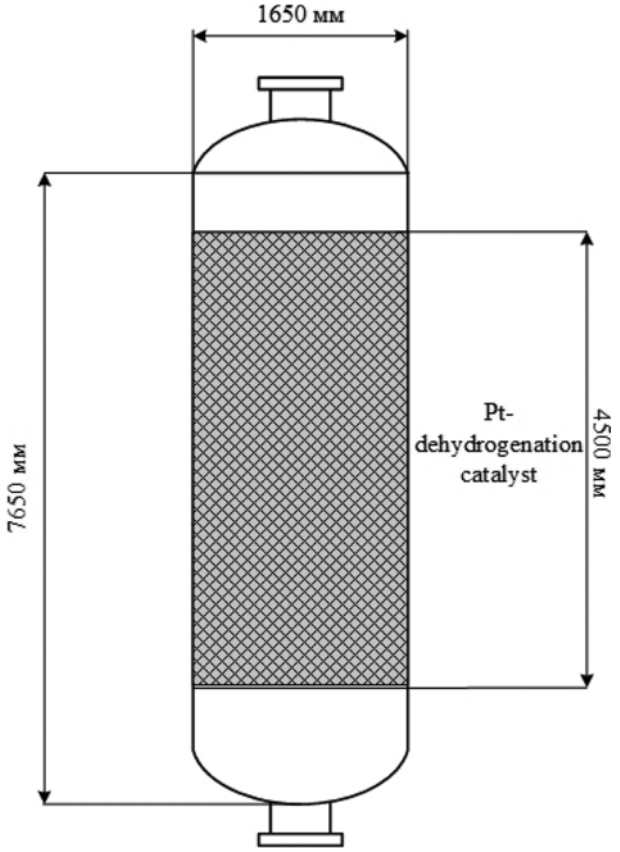

Fig. 1. The scheme of the reactor for dehydrogenation of paraffins of middle distillate fractions (C_9-C_{14}).

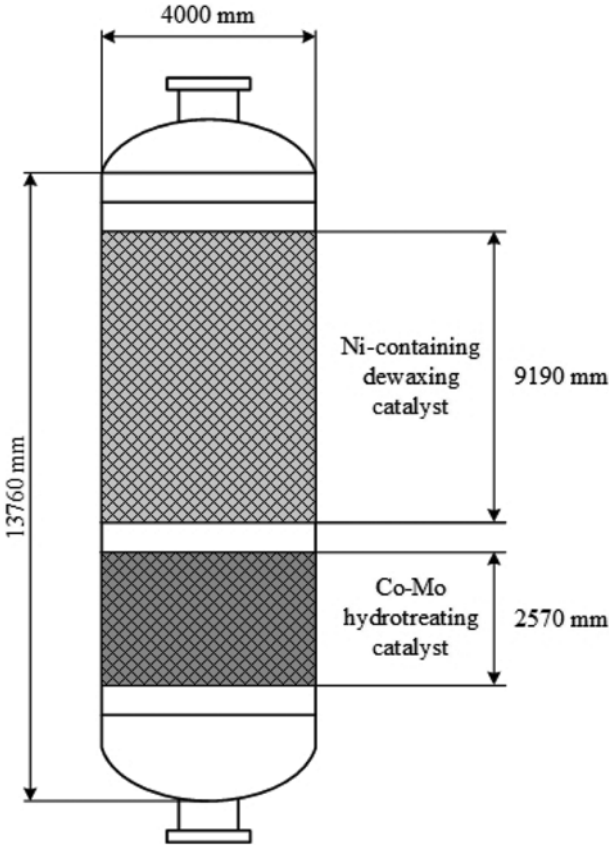

Fig. 2. The scheme of the reactor for dewaxing of paraffins of the middle distillate fractions (C_5-C_{27}).

Table 1. Composition and properties of the feedstock of the dehydrogenation process

Component	Feedstock 1	Feedstock 2	Feedstock 3
Nonan C_9H_{20}	0.02	0.08	0.02
Decane $C_{10}H_{22}$	11.19	16.02	10.96
Undecane $C_{11}H_{24}$	35.77	31.52	32.49
Hendecane $C_{12}H_{26}$	30.41	27.77	29.35
Tridecane $C_{13}H_{28}$	19.32	21.82	23.82
Tetradecane $C_{14}H_{30}$	0.33	0.4	0.39
Circulating linear alkyl benzene (LAB)	0.95	0.83	0.91
Residuum (isoparaffins and aromatics)	0.12	0.11	0.13
Feedstock properties			
Density (ρ), kg/m^3	750	750	750

Table 2. Composition and properties of hydrogenous gas of the dehydrogenation process

Components	%vol
Hydrogen	92.03
Methane	1.73
Ethane	3.66
Propane	1.61
Butane	0.47
Pentane and>	0.11
Nirogen	0.39
Σ	100
Properties of hydrogenous gas	
Density (ρ), kg/m^3	147

(the height is 13,760 mm, the diameter is 4,000 mm). The main purpose of the process is to obtain diesel fraction by removing long chain paraffins (C_5-C_{27}) [31-33]. The conversion of the process comprises 95% at the selectivity to the diesel fraction of 58-63%.

2. Feedstock and Hydrogenous Gas Specifications

The feedstock of dehydrogenation and dewaxing processes of hydrocarbons of middle distillate fractions, as well as hydrogenous gas were taken from industrial units. The composition and the properties of the feedstock, as well as, hydrogenous gas are presented in Table 1-4.

3. Technological Conditions

The values of technological parameters, that have significant influence on the process of dehydrogenation, such as temperature, feedstock flow rate, hydrogen/feedstock molar ratio are presented in Table 5. The pressure in the reactor was maintained at the constant rate corresponding to the value of 0.2 MPa. The values of technological parameters of the dewaxing process, such as temperature, feedstock flow rate, hydrogenous gas consumption, are presented in Table 6. The pressure in the dewaxing reactor was constant and corresponded to 7.0 MPa.

METHOD OF RESEARCH

Mathematical modelling was applied in the current research. Mathematical models of the dehydrogenation [34] and dewaxing [35] processes, based on the activity of the catalyst, which are the systems of equations of material and heat balances for each component of the formalized scheme of hydrocarbon transformations, were used:

$$\begin{cases} G\cdot\dfrac{\partial C_i}{\partial z}+G\cdot\dfrac{\partial C_i}{\partial V}=\sum_{j=1}^{m}a_j\cdot W_j \\ G\cdot\dfrac{\partial T}{\partial z}+G\cdot\dfrac{\partial T}{\partial V}=\dfrac{1}{\rho\cdot C_p^{mix}}\sum_{j=1}^{m}Q_j\cdot a_j\cdot W_j \end{cases} \quad (1)$$

Table 3. Composition and properties of the feedstock of the dewaxing proces

Components	Feedstock 1	Feedstock 2	Feedstock 3	Feedstock 4	Feedstock 5
n-Paraffins (C_{10}-C_{27})	16.12	17.09	16.46	14.86	19.19
n-Paraffins (C_5-C_9)	0.69	0.58	2.22	0.6	1.15
Olefins	1.09	2.10	0.45	1.98	2.50
Naphthenes	29.19	35.00	38.34	39.85	38.91
i-Paraffins	30.00	24.36	21.89	22.70	18.25
Monoaromatic hydrocarbons	21.68	19.68	19.4	18.82	18.82
Polyaromatic hydrocarbon	1.23	1.09	1.2	1.12	1.12
Hydrogen sulphide	0.0016	0.0975	0.0333	0.0703	0.0555
Properties of feedstock					
Cloud point, °C	−1 °C	−11 °C	−7 °C	−8 °C	−6 °C
Freezing point, °C	−11 °C	−20 °C	−17 °C	−7 °C	−15 °C

Table 4. Composition and properties of hydrogenous gas of the dewaxing process

Components	%wt
Hydrogen	42.30
Methane	17.46
Ethane	13.13
Propane	11.93
n-Butane	4.11
i-Butane	5.20
n-Pentane	0.90
i-Pentane	1.95
Paraffins C_{6+}	0.90
Hydrogen sulphide	2.12
Properties of feedstock	
Density (ρ), kg/m^3	147

Table 5. Operating conditions of the dehydrogenation process

Operating condition	
Reactor inlet temperature, °C	470-490
Feedstock flow rate, m^3/h	75
Hydrogen/Feedstock molar ratio	6.0/1.0-8.5/1.0

Table 6. Operating conditions of the dewaxing process

Operating condition	
Reactor inlet temperature, °C	330-360
Feedstock flow rate, m^3/h	240-280
Hydrogen flow rate, Nm^3/h	10000-50000

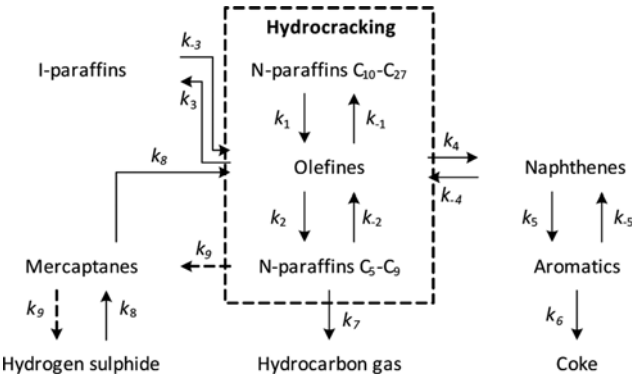

Fig. 4. The formalized conversion reaction network of the dewaxing process.

Initial conditions: z=0: $C_i=C_{i,0}$; $T=T_0$; V=0: $C_i=C_{i,0}$; $T=T_0$, where z is the volume of refined feedstock from the moment of fresh catalyst load, m^3; G is the feedstock flow rate, m^3/h; z=G·t (t is the catalyst operating time from the moment of fresh catalyst load, h); C_i is the content of i^{th} component, mol/*l*; V is the catalyst bed volume, m^3; a_j is the catalyst activity in j^{th} reaction; ρ is the density of mixture, kg/m^3; C_p^{mix} is the specific heat capacity of the mixture, J/(kg·K); Q_j is the heat effect of j^{th} reaction, J/mol; T is the temperature, K; W_j is the rate of j^{th} reaction, mol/(*l*·s); m is the number of reactions.

For the mathematical description of hydrodynamic and heat and mass transfer regimes of the industrial dehydrogenation reactor and the industrial dewaxing reactor the following assumptions were accepted:

- the industrial reactor is considered an ideal plug flow reactor;

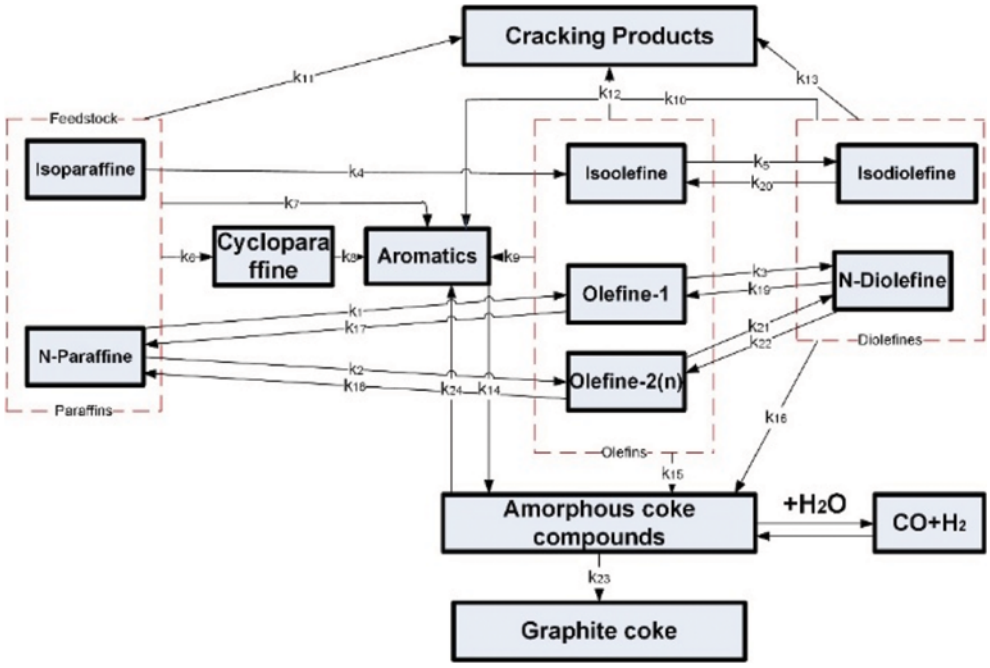

Fig. 3. The formalized reaction network of the paraffins dehydrogenation process with reversible oxidation of amorphous coke compounds by water.

Table 7. Values of the main kinetic parameters of paraffins dehydrogenation process

Reaction	Kinetic parameter of the reaction	
	E_a, kJ/mol	k_0
N-Paraffin→Olefin-1+H_2	110	$7.45 \cdot 10^7$ s^{-1}
N-Paraffin→Olefin-2(n)+H_2	118	$8.03 \cdot 10^7$ s^{-1}
Olefin-1+H_2→N-Paraffin	60	$3.92 \cdot 10^3$ $l \cdot s^{-1} \cdot mol^{-1}$
Olefin-2(n)+H_2→N-Paraffin	85	$5.45 \cdot 10^3$ $l \cdot s^{-1} \cdot mol^{-1}$
Olefin-1→N-Diolefin+H_2	190	$2.65 \cdot 10^{11}$ s^{-1}
Olefin-2(n)→N-Diolefin+H_2	190	$2.65 \cdot 10^{11}$ s^{-1}
N-Diolefin+H_2→Olefin-1	160	$5.55 \cdot 10^9$ $l \cdot s^{-1} \cdot mol^{-1}$
N-Diolefin+H_2→Olefin-2(n)	160	$4.18 \cdot 10^9$ $l \cdot s^{-1} \cdot mol^{-1}$
Isoparaffin→Isoolefin+H_2	170	$2.10 \cdot 10^{11}$ s^{-1}
Isoolefin→Isodiolefin+H_2	150	$8.30 \cdot 10^8$ s^{-1}
Isodiolefin+H_2→Isoolefin	115	$3.28 \cdot 10^6$ $l \cdot s^{-1} \cdot mol^{-1}$
Paraffin→Cycloparaffin+H_2	200	$5.20 \cdot 10^{10}$ s^{-1}
Paraffin→Aromatic Compounds+4H_2	140	$1.10 \cdot 10^8$ s^{-1}
Olefin→Aromatic Compounds+3H_2	135	$1.40 \cdot 10^8$ s^{-1}
N-Dien→Aromatic Compounds+2H_2	135	$2.00 \cdot 10^8$ s^{-1}
Cycloparaffin→Aromatic Compounds+3H_2	160	$9.00 \cdot 10^{10}$ s^{-1}
Paraffin→Cracking product	200	$1.00 \cdot 10^{10}$ s^{-1}
Olefin→Cracking product	200	$1.00 \cdot 10^{10}$ s^{-1}
N-Diolefin→Cracking product	200	$1.00 \cdot 10^{10}$ s^{-1}
Aromatic Compounds→Amorphous coke compounds	220	$5.50 \cdot 10^{10}$ s^{-1}
Amorphous coke compounds+H_2→Aromatic Compounds	250	$2.40 \cdot 10^8$ s^{-1}
Amorphous coke compounds+H_2O→CO+H_2	160	$8.60 \cdot 10^{12}$ s^{-1}
Olefin→Amorphous coke compounds	220	$4.80 \cdot 10^{10}$ s^{-1}
N-Diolefin→Amorphous coke compounds	220	$5.00 \cdot 10^{10}$ s^{-1}
Amorphous coke compounds→Graphite coke	180	$1.00 \cdot 10^{10}$ s^{-1}

- mass and heat transport occurs by means of convection;
- the basis for the developed mathematical models are the formalized hydrocarbon conversion scheme (Fig. 3, Fig. 4).

The dehydrogenation reactor is a fixed bed reactor, in which Pt-catalyst is loaded (Fig. 1) It is a capacitive device with a radial entering of the feedstock. The overall dimensions of the reactor are: diameter of 1,650 mm, and height of 7,650 mm. In this case, the application of the ideal plug flow model is possible to describe the paraffin dehydrogenation process in a fixed-bed reactor. According to the calculation of the Peclet number (Pe=2494, Pe_T/Pe_D= 1.05-1.5), we can assume that diffusion plays an insignificant role in the process of mass and heat transfer by means of convection. The reaction-limited regime is observed for the dehydrogenation process (Thiele modulus Φ_j<1, internal effectiveness factor η_j= 0.98-1.00). The parameters of the model of dehydrogenation process are presented in Table 7.

The dewaxing reactor is a vertical apparatus with axial flow of feedstock. The scheme of the reactor is presented in Fig. 2. The overall dimensions of the reactor are: diameter of 4,000 mm, height of 13,760 mm. The volumes of the loaded dewaxing and hydrotreating catalysts are 115 m^3 and 22 m^3, respectively. The application of the ideal plug flow model is appropriate to describe the dewaxing process in the fixed-bed reactor. According to the Peclet number (Pe=26681, Pe_T/Pe_D=1.05-1.50) it can be assumed that diffusion plays an insignificant role in the process of mass and heat transfer, which occurs by means of convection. For the dewaxing process, a reaction limited regime is observed (Thiele modulus Φ_j<1, internal effectiveness factor η_j=0.98-1.00). The parameters of the model of dewaxing process are presented in Table 8.

Table 8. The values of the kinetic parameters of dewaxing and hydrotreating processes

No.	Reaction	Kinetic parameter of the reaction	
		E_a, kJ/mol	k_0
Dewaxing process			
1.	N-paraffins dehydrogenation	110	$4.12 \cdot 10^9$
2.	Hydrocracking of olefins	140	$1.04 \cdot 10^6$
3.	Olefin isomerization and hydrogenation	130	$6.07 \cdot 10^8$
4.	Olefin cyclization	180	$6.47 \cdot 10^{10}$
5.	Naphthenes dehydrogenation	140	$3.70 \cdot 10^3$
6.	Coke formation	190	$2.39 \cdot 10^{12}$
7.	N-paraffins cracking	200	$1.10 \cdot 10^7$
8.	Mercaptan formation	80	$2.95 \cdot 10^6$
Hydrotreating process			
9.	Mercaptan hydrogenation	80	$3.67 \cdot 10^7$

Reaction rate constants were obtained by solving the inverse kinetic problem, so having data about product outputs at the dehydrogenation process conditions (temperature, pressure, feedstock flow rate), rate constants were determined to obtain their best rating in terms of minimizing the following functional:

$$\hat{O}(K(x, t)) = \sum_{l}(C(x, t) - z_1(x, t))^2, \quad (2)$$

where $z_1(x, t)$ - the product of distribution function observed in experiment 1; C(x, t) - hydrocarbon concentration distribution at the time t, calculated by the equations of the model; x - the serial number of the hydrocarbon; t - time.

The optimal amount of water in the process of dehydrogenation is calculated from the thermodynamic conditions of the equilibrium shift in the reaction of oxidation of intermediate products of condensation (the coke of amorphous structure) by water:

$$C_{28}H_{14} + 28H_2O \rightleftarrows 28CO + 35H_2$$

according to the following equations:

$$\begin{cases} \dfrac{K_{i+1}}{K_i} = \left(\dfrac{n^*_{CO(i+1)}}{n^*_{CO(i)}}\right)^{63} \cdot \left(\dfrac{n_{iH_2O} - n^*_{CO(i)}}{n_{H_2O(i+1)} - n^*_{CO(i+1)}}\right)^{28} \\ \qquad \cdot \left(\dfrac{n_{iH_2O} + 1.25n^*_{CO(i)}}{n_{H_2O(i+1)} + 1.25n^*_{CO(i+1)}}\right)^{35} = 1 \\ K_p = -\dfrac{(\Delta H_r - T \cdot \Delta S_r)}{RT} \end{cases}, \quad (3)$$

where K_p - the equilibrium constant at the temperature of the process, Pa; T - the temperature of the process, K; R=8.31 J/(mol K) - the gas constant; ΔH_r - the enthalpy change of the reaction at the temperature T, J/mol; ΔS_r - the entropy change of the reaction at the temperature of the process, J/(mol K); K_{i+1} - the equilibrium constant at T_{i+1}, Pa[21]; K_i - the equilibrium constant at T_i, Pa[21]; $n_{H_2O(i+1)}$ - the initial amount of H_2O at T_{i+1}, mol; n_{iH_2O} - the initial amount of H_2O at T_i, mol; $n^*_{CO(i+1)}$ - the equilibrium amount of CO at T_{i+1}, mol; $n^*_{CO(i)}$ - the equilibrium amount of CO at T_i, mol; $(n_{H_2O(i+1)} - n^*_{CO(i+1)})$ - the equilibrium amount of H_2O at T_{i+1}, mol; $(n_{iH_2O} - n^*_{CO(i)})$ - the equilibrium amount of H_2O at T_i, mol; $(n_{H_2O(i+1)} + 1.25n^*_{CO(i+1)})$ - the equilibrium amount of H_2 at T_{i+1}, mol; $(n_{iH_2O} + 1.25n^*_{CO(i)})$ - the equilibrium amount of H_2 at T_i, mol.

Thermodynamic parameters of this reaction at temperature 480 °C were calculated (ΔG_r=−50.84 kJ/mol, ΔH_r=145 kJ/mol, ΔS_r= 0.26 kJ/(mol K). The value obtained for the free energy (ΔG_r= −50.84 kJ/mol) suggests that this reaction is thermodynamically feasible under the operating conditions of the dehydrogenation process.

These features of change in the conversion of amorphous coke in its oxidation reaction with water formed the basis for an applied procedure that makes it possible to calculate the optimal rate of water supply to the reactor depending on the temperature. The method, developed by the authors, was published in the earlier works [36,37].

Calculation error of the models does not exceed 5%, which is comparable to the error of the method of chromatography analysis used to determine the content of hydrocarbons. The mathematical models of the processes of dehydration and dewaxing were implemented into software using the programming language Pascal.

RESULTS AND DISCUSSION

Using the mathematical model of the process of dehydrogenation of hydrocarbons of middle distillate fractions (C_9-C_{14}), the influence of the hydrogen/feedstock molar ratio on the main indicators of the process, such as the yield of the target products (olefins), the yield of the by-products (diolefins), and the coke formation dynamics on the Pt-catalyst, was studied. The study was carried out at various temperatures corresponding to the beginning (470 °C), the middle (480 °C) and the end (490 °C) of the production cycle of the process, the pressure of 0.2 MPa, the feedstock flow rate of 75 m^3/h for three different compositions of the feedstock (Table 2) and hydrogenous gas (Table 3). The results of the study are shown in Figs. 5-13. Thus, the results showed that when the hydrogen/feedstock ratio is reduced from 8.5/1.0 to 6.0/1.0 in the temperature range from 470 to 490 °C, the yield of unsaturated hydrocarbons (olefins and diolefins) and coke increase along the entire length of the production cycle of the dehydrogenation process. Moreover, the higher the temperature, the more significant this effect

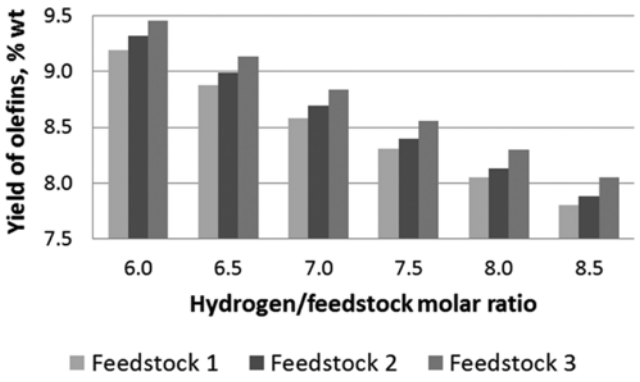

Fig. 5. The yield of olefins in dehydrogenation of hydrocarbons of middle distillate fractions (C_9-C_{14}) at the change of hydrogen/feedstock molar ratio at the beginning of operational cycle (470 °C).

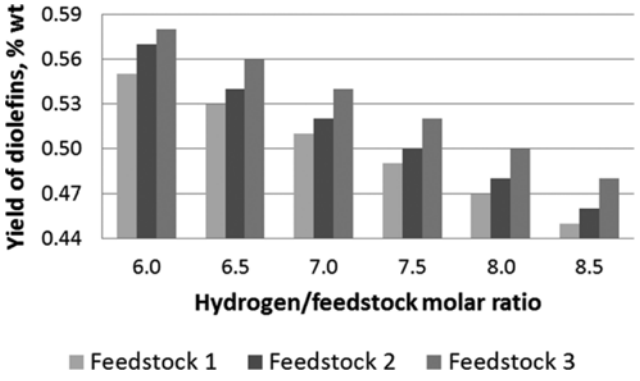

Fig. 6. The yield of diolefins in dehydrogenation of hydrocarbons of middle distillate fractions (C_9-C_{14}) at the change of hydrogen/feedstock molar ratio at the beginning of operational cycle (470 °C).

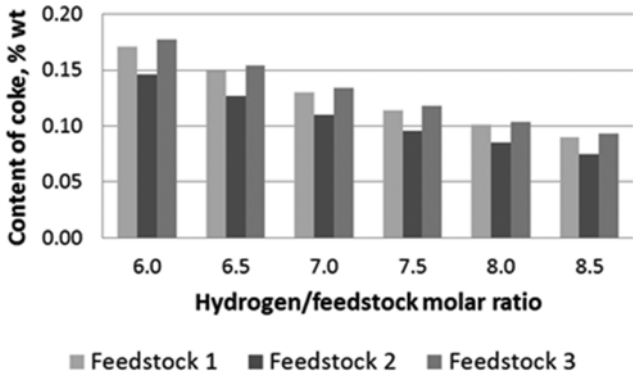

Fig. 7. The content of coke in dehydrogenation of hydrocarbons of middle distillate fractions (C_9-C_{14}) at the change of hydrogen/feedstock molar ratio at the beginning of operational cycle (470 °C).

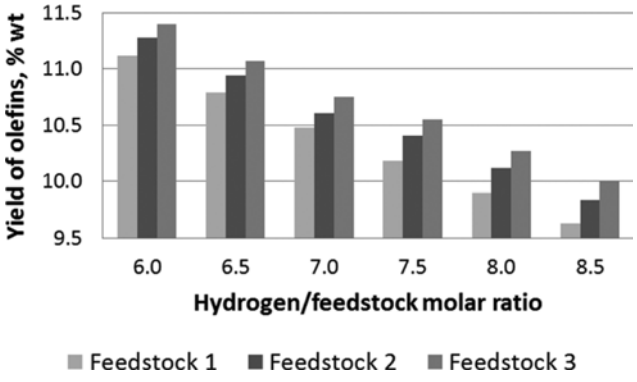

Fig. 8. The yield of olefins in dehydrogenation of hydrocarbons of middle distillate fractions (C_9-C_{14}) at the change of hydrogen/feedstock molar ratio at the middle of operational cycle (480 °C).

is, which is associated with the endothermic effect of the dehydrogenation reactions and the shift of the equilibrium of these reactions towards the products, leading to an increase in conversion. So, at the beginning of the production cycle of the dehydrogenation process, the reduction of the hydrogen/feedstock molar ratio from 8.5/1.0 to 6.0/1.0 at the temperature of 470 °C leads to an increase in the yield of olefins by an average of 1.4%wt (Fig. 5), diolefins by 0.10%wt (Fig. 6), coke by 0.07-0.08%wt (Fig. 7), respectively. As the temperature in the reactor increases up to 480 °C in the middle of the production cycle of the process, the decrease in the hydrogen/feedstock molar ratio from 8.5/1.0 to 6.0/1.0 exerts greater influence on the yield of unsaturated hydrocarbons and coke: the yield of olefins increases by an average of 1.45%wt (Fig. 8), diolefins by 0.13%wt (Fig. 9), coke by 0.1%wt (Fig. 10), respectively. At the end of the production cycle of the dehydrogenation process, at 490 °C the decrease in the hydrogen/feedstock molar ratio from 8.5/1.0 to 6.0/1.0 leads to an increase in the yield of olefins on average (depending on the composition of the feedstock) by 1.55%wt (Fig. 11), diolefins by 0.15%wt (Fig. 12), coke by 0.18%wt (Fig. 13), respectively. Thus, as the temperature rises from 470 to 490 °C and the hydrogen/feedstock ratio decreases from 8.5/1.0 to

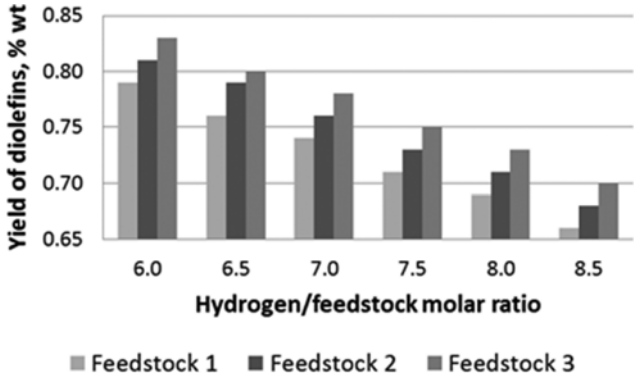

Fig. 9. The yield of diolefins in dehydrogenation of hydrocarbons of middle distillate fractions (C_9-C_{14}) at the change of hydrogen/feedstock molar ratio at the middle of operational cycle (480 °C).

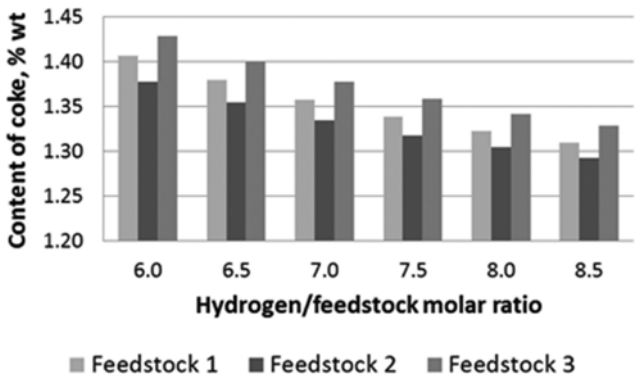

Fig. 10. The content of coke in dehydrogenation of hydrocarbons of middle distillate fractions (C_9-C_{14}) at the change of hydrogen/feedstock molar ratio at the middle of operational cycle (480 °C).

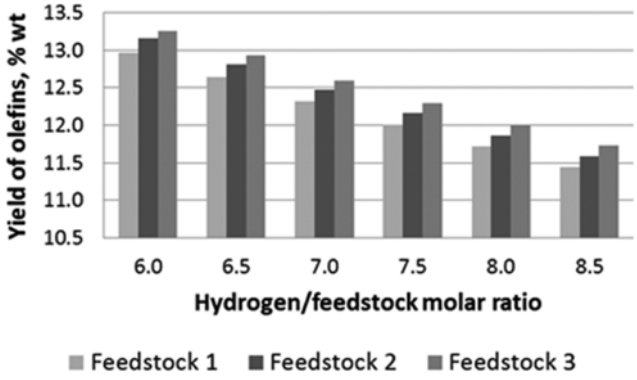

Fig. 11. The yield of olefins in dehydrogenation of hydrocarbons of middle distillate fractions (C_9-C_{14}) at the change of hydrogen/feedstock molar ratio at the end of operational cycle (490 °C).

6.0/1.0, the olefin yield increases by 1.45-1.55%wt (Fig. 5, 8, 11), the yield of diolefins increases by 0.1-0.15%wt (Fig. 6, 9, 12), the coke yield increases by 0.07-0.18%wt depending on the feedstock composition (Fig. 7, 10, 13).

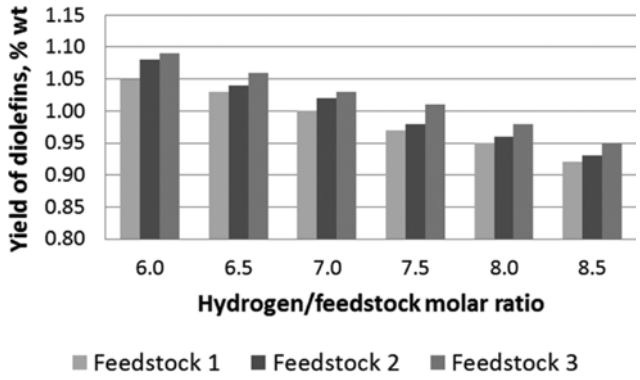

Fig. 12. The yield of diolefins in dehydrogenation of hydrocarbons of middle distillate fractions (C_9-C_{14}) at the change of hydrogen/feedstock molar ratio at the end of operational cycle (490 °C).

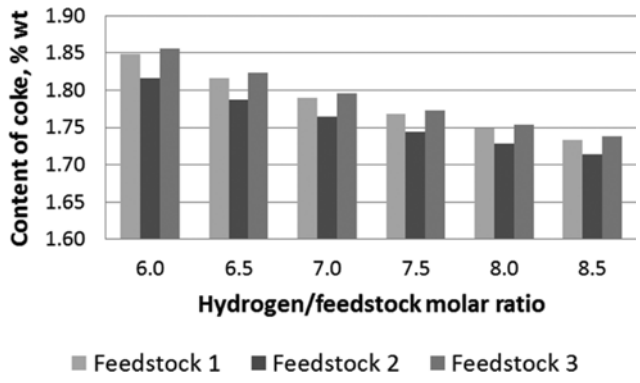

Fig. 13. The content of coke in dehydrogenation of hydrocarbons of middle distillate fractions (C_9-C_{14}) at the change of hydrogen/feedstock molar ratio at the end of operational cycle (490 °C).

Such decrease of the hydrogen/feedstock molar ratio during the dehydrogenation process allows increasing the yield of olefins by 1.45-1.55%wt and reduces the hydrogen consumption by 25,000 Nm^3/h (at the decrease in the hydrogen/feedstock molar ratio from 8.5/1.0 to 6.0/1.0) in order to use it in the process of dewaxing.

However, the decrease in the molar ratio of hydrogen/feedstock to the 6.0/1.0 level at the dehydrogenation unit leads to the intensification of coke formation on the platinum catalyst almost twofold (Fig. 7, 10, 13) for different feedstock compositions, which leads to its faster deactivation. To compensate for this effect, the dynamics of the water flow rate (Fig. 14) in the dehydrogenation reactor was determined as a function of the process temperature based on the method developed by the authors [36]. In these thermodynamic conditions, water interacts with the intermediate products of condensation, oxidizing them and preventing from transition to a graphite state [37], which allows slowing down coke formation on the catalyst and prevent its rapid deactivation.

Calculations of water flow rate in the dehydrogenation reactor were carried out in the temperature range of the process from 470 °C to 490 °C, pressure of 0.2 MPa, feedstock flow rate of 75 m^3/h, the hydrogen/feedstock molar ratio of 6.0/1.0, due to the predetermined olefin yield of 9.68% for different feedstock composition (Table 2). The results of calculating the coke formation during the water flow supply depending on the temperature of the process and the feedstock composition are shown in Fig. 15. The results of calculations showed that an increase in water flow rate with increasing temperature in the reactor makes it possible to reduce coke formation caused by the decrease in the hydrogen/feedstock molar ratio from 8.5/1.0 to 6.0/1.0 to slow deactivation and prolong its service life. So, when supplying water, for feedstock 1 the coke concentration at the end of the cycle is 1.25%wt, for feedstock 2 the coke concentration is 1.44%wt, for feedstock 3 the coke concentration is 1.56%wt (Fig. 15), which is by 0.3-0.6%wt lower than the operation of the catalyst without water supply.

The obtained results allow us to conclude that it is reasonable to

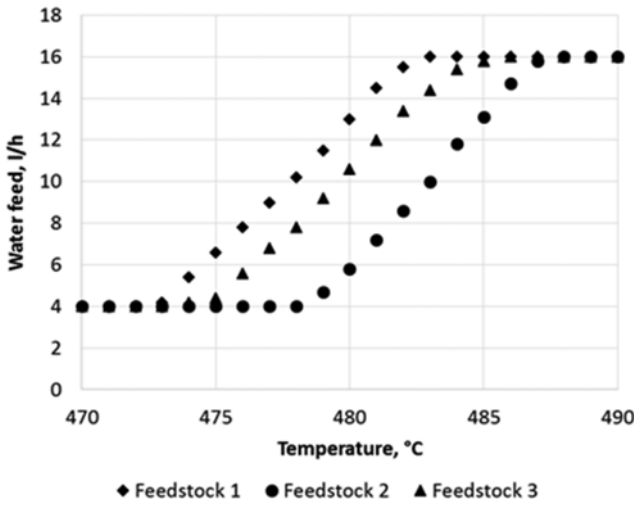

Fig. 14. The dynamics of water supply depending on the temperature of the dehydrogenation process at the hydrogen/feedstock molar ratio 6.0/1.0 for different feedstock composition at the predetermined yield of olefins of 9.68%wt.

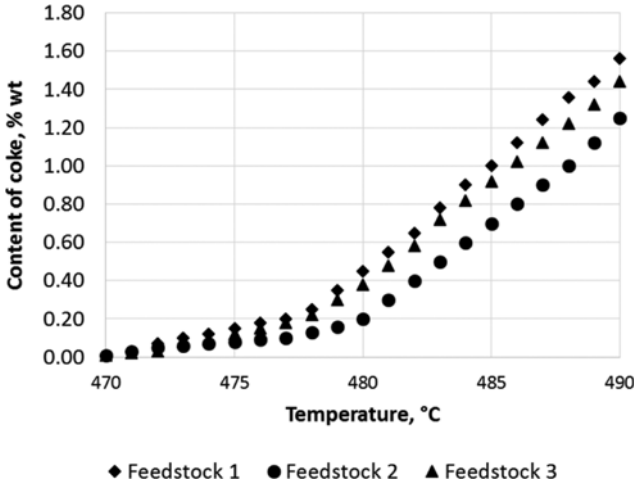

Fig. 15. The dynamics of coke accumulation depending on the temperature of the dehydrogenation process at the hydrogen/feedstock molar ratio 6.0/1.0 for different feedstock composition at the predetermined yield of olefins of 9.68%wt.

decrease the hydrogen/ feedstock molar ratio in the dehydrogenation unit from 8.5/1.0 to 6.0/1.0, having increased the olefin yield by 1.45-1.55%wt, and to reduce hydrogen consumption by 25,000 Nm^3/h for directing it to the middle distillate fractions dewaxing unit. However, it is necessary to increase the water flow rate in the dehydrogenation reactor to compensate for the intensification of coke formation reactions by oxidation of the intermediate products of condensation. The increase in water flow rate provides the decrease in the dynamics of coke accumulation, so that at the end of the cycle, the concentration of coke on the surface will be on average 0.3-0.6%wt lower, which will allow maintaining the optimum catalyst activity for longer time and extend its service life.

The effect of hydrogen flow rate on the efficiency of the dewaxing process was assessed by using a mathematical model under the following conditions: the pressure of 7.0 MPa, the temperatures of 300 °C and 340 °C corresponding to the beginning and end of the cycle of the unit, respectively, the feedstock flow rate of 240 m^3/h, the hydrogenous gas flow rate was varied from 10,000 to 50,000 Nm^3/h. At the same time, the yield of the diesel fraction and the main quality indicator (freezing point and cloud point) were estimated. The results of the study are shown in Figs. 16-19.

The results of the study showed that the cloud point and the freezing point of the obtained product (diesel fraction) are reduced for different feedstock compositions with an increase in hydrogenous gas consumption during the catalytic dewaxing of middle distillate fractions. Thus, with an increase in the hydrogenous gas consumption from 10,000 to 50,000 Nm^3/h at the reactor temperature of 300 °C, corresponding to the beginning of the operating cycle of the unit with fresh catalyst, the cloud point and the freezing point of the diesel fraction decrease by 1-4 °C (Fig. 16, 17), and this tendency is typical of all feedstock compositions. Closer to the end of the operating cycle at the reactor temperature of 340 °C, the effect of hydrogenous gas consumption on the low-temperature properties of the diesel fraction becomes more significant. Thus, with an increase in the consumption of hydrogenous gas consumption from 10,000 to 50,000 Nm^3/h the cloud point and the freezing point are reduced by 11-25 °C for feedstock No. 1, by 3-12 °C for feedstock No. 2, by 12-20 °C for feedstock No. 3, by 6-20 °C for feedstock No. 4, by 6-21 °C for feedstock No. 5, respectively (Fig. 18, 19). The decrease of the cloud point and the freezing point of the product (diesel fraction) with increasing of the hydrogenous gas consumption in the catalytic dewaxing reactor is associated with the intensification of hydrocracking reaction, leading to the formation of lighter hydrocarbons with low cloud and freezing point [38-40]. The studies showed that an increase in the hydroge-

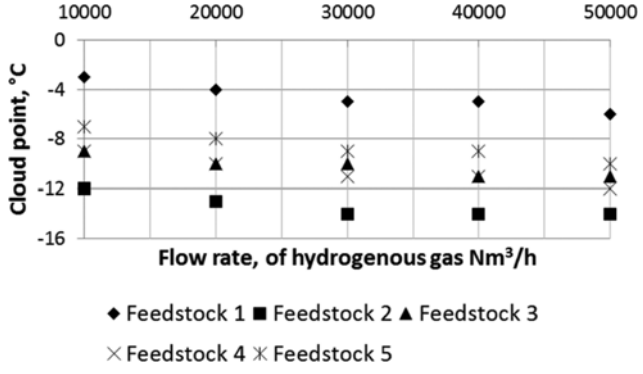

Fig. 16. The dependency of the cloud point of diesel fraction on the hydrogenous gas consumption at the temperature in the dewaxing reactor of 300 °C for different feedstock compositions.

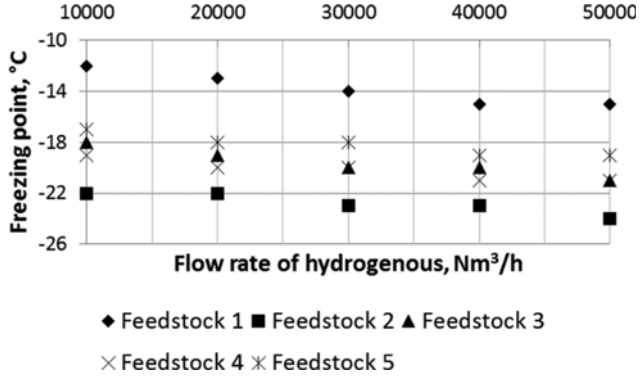

Fig. 17. The dependency of the freezing point of diesel fraction on the hydrogenous gas consumption at the temperature in the dewaxing reactor of 300 °C for different feedstock compositions.

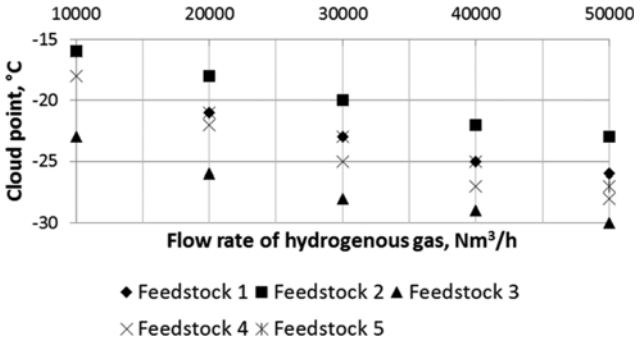

Fig. 18. The dependency of the cloud point of diesel fraction on the hydrogenous gas consumption at the temperature in the dewaxing reactor of 340 °C for different feedstock compositions.

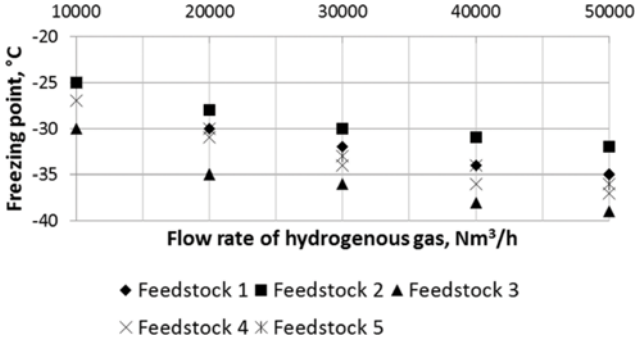

Fig. 19. The dependency of the freezing point of diesel fraction on the hydrogenous gas consumption at the temperature in the dewaxing reactor of 340 °C for different feedstock compositions.

nous gas consumption in the dewaxing reactor affects the low-temperature properties of the diesel fraction: with an increase in the hydrogenous gas consumption from 10,000 to 50,000 Nm^3/h, low-temperature properties of the diesel fraction are improved, i.e., the cloud point and the freezing point of the resulting diesel fraction are reduced by 1-4 °C and 10-25 °C (at 300 °C and 340 °C, respectively). The higher the process temperature the more significant this effect is, which is associated with the intensification of hydrocracking reaction leading to the formation of lighter hydrocarbons with low cloud point and freezing point.

CONCLUSIONS

1. Decrease of the hydrogen/feedstock molar ratio from 8.5/1.0 to 6.0/1.0 in the process of dehydrogenation of paraffins of middle distillate fractions (C_9-C_{14}) allows increasing the conversion level of the process due to the shift of thermodynamic equilibrium of the target reaction (dehydrogenation of paraffins to olefins) and increasing the yield of olefins by 1.45-1.55%wt. Herewith, the yield of by-products increases insignificantly: the yield of diolefins increases by 0.10-0.15%wt, the yield of coke increases by 0.07-0.18%wt depending on the feedstock composition.

2. Water supply to the reactor of dehydrogenation of paraffins of middle distillate fraction (C_9-C_{14}) makes it possible to compensate the intensification of coke formation caused by decreasing the hydrogen/feedstock molar ratio from 8.5/1.0 to 6.0/1.0 due to the oxidation of the intermediate products of condensation. When water is supplied by increasing portions with increasing temperature, the content of coke on the catalyst at the end of the cycle is 1.25-1.56%wt depending on the feedstock composition, which is by 0.3-0.6%wt lower than during working without water.

3. Decrease of the hydrogen/feedstock molar ratio from 8.5/1.0 to 6.0/1.0 at the dehydrogenation unit provides additional amount of hydrogenous gas (25,000 Nm^3/h). Utilization of this excess amount of hydrogenous gas at the dewaxing unit allows increasing the depth of conversion in the reaction of hydrocracking of long-chain paraffins of middle distillate fractions with the formation of lighter hydrocarbons having low cloud point and freezing point, and, consequently, improving low-temperature properties of obtained diesel fraction. The cloud point and freezing point of obtained diesel fraction decrease by 1-4 °C and 10-25 °C (at the temperature 300 °C and 340 °C respectively).

4. The studies, carried out using mathematical models of the dehydrogenation and dewaxing processes of the middle distillate fractions, showed that intensification of these processes is achieved due to redistribution of hydrogen between the two units at the same operation costs. Thus, the decrease in the hydrogen/feedstock molar ratio from 8.5/1.0 to 6.0/1.0 in the dehydrogenation unit allows increasing the yield of olefins by 1.45-1.50%wt and decreasing hydrogenous gas consumption by 25,000 Nm^3/h. The use of additional amounts of hydrogen from the dehydrogenation unit at the dewaxing unit allows the diesel fraction to be obtained with the improved low-temperature properties: the cloud point and the freezing point of the resulting diesel fraction are reduced by 1-4 °C and 10-25 °C (at the temperature of 300 °C and 340 °C respectively).

NOMENCLATURE

- Z : the amount of recycled materials since loading of fresh catalyst [m^3; $z=G\cdot t$]
- G : flow rate of feedstock [m^3/hour]
- t : operating time of catalyst since loading of fresh catalyst [h]
- C_i : concentration of i-component [mol/*l*]
- V : volume of catalyst layer [m^3]
- a_j : activity of catalyst in the j-th reaction
- ρ : density of the mixture [kg/m^3]
- C_p^{mix} : specific heat of the mixture [j/(kg (K))]
- Q_j : thermal effect of the j-th reaction [j/mol]
- T : temperature [K]
- W_j : rate of j-th reaction [mol/(litre s)]
- m : the number of reactions
- E_a : activation energy [kJ/mol]
- k_0 : rate constant [$s^{-1}/s^{-1}\cdot mol^{-1}$]
- Pe : peclet number
- Pe_T : heat peclet number
- Pe_D : diffusion peclet number
- Φ_j : thiele modulus
- η_j : internal effectiveness factor
- $\hat{O}$ (K(x, t)) : optimization function
- $z_1(x, t)$: the product of distribution function observed in experiment 1
- C(x, t) : hydrocarbon concentration distribution at time t, calculated by the equations of the model
- x : the serial number of the hydrocarbon
- t : time [s]
- K_p : the equilibrium constant at T [Pa]
- R : 8.31 J/(mol K) - the gas constant
- ΔG_r : the free energy change of the reaction at a temperature T [J/mol]
- ΔH_r : the enthalpy change of the reaction at a temperature T [J/mol]
- ΔS_r : the entropy change of the reaction at a temperature T [J/(mol K)]
- K_{i+1} : the equilibrium constant at T_{i+1} [Pa^{21}]
- K_i : the equilibrium constant at T_i [Pa^{21}]
- $n_{H_2O(i+1)}$: the initial amount of H_2O at T_{i+1} [mol]
- n_{iH_2O} : the initial amount of H_2O at T_i [mol]
- $n^*_{CO(i+1)}$: the equilibrium amount of CO at T_{i+1} [mol]
- $n^*_{CO(i)}$: the equilibrium amount of CO at T_i [mol]
- $(n_{H_2O(i+1)} - n^*_{CO(i+1)})$: the equilibrium amount of H_2O at T_{i+1} [mol]
- $(n_{iH_2O} - n^*_{CO(i)})$: the equilibrium amount of H_2O at T_i [mol]
- $(n_{H_2O(i+1)} + 1.25n^*_{CO(i+1)})$: the equilibrium amount of H_2 at T_{i+1} [mol]
- $(n_{iH_2O} + 1.25n^*_{CO(i)})$: the equilibrium amount of H_2 at T_i [mol]

ACKNOWLEDGEMENTS

The Ministry of Education and Science of the Russian Federation (10.8306.2017/6.7) supported the research. The research is carried out at National Research Tomsk Polytechnic University and within the framework of National Research Tomsk Polytechnic University Competitiveness Enhancement Program grant.

REFERENCES

1. J. G. Speight, *The Refinery of the Future*, Elsevier (2011).
2. D. Stratiev and K. Petkov, *Hydrocarbon Process.*, **88**(9), 93 (2009).
3. G. Phillips and F. Liu, *Hydrocarbon Eng.*, **8**(9), 63 (2003).
4. M. S. Rana, V. Sámano, J. Ancheyta and J. A. I. Diaz, *Fuel*, **86**(9), 1216 (2007).
5. P. Leprince, *Petroleum refining. Volume 3. Conversion Processes*, Editions Technip (2000).
6. D. S. J. Jones and P. R. Pujado, *Handbook of Petroleum Processing*, Springer (2006).
7. M. R. Riazi, *Characterization and Properties of Petroleum Fractions*, ASTM manual series (2005).
8. J. Ancheyta, A. Alvarez-Majmutov and C. Leyva, *Hydrotreating of oil fractions: Multiphase Catalytic Reactors: Theory, Design, Manufacturing, and Applications*, John Wiley & Sons, Inc, New Jersey, Canada (2016).
9. I. Sharafutdinov, D. Stratiev, I. Shishkova, R. Dinkov, A. Batcharov, P. Petkov and N. Rudnev, *Fuel*, **96**, 556 (2012).
10. A. L. Lown, L. Peerboom, S. Mueller, J. Anderson, D. Miller and C. Lira, *Fuel*, **117**, 544 (2014).
11. A. Anwar and A. Garforth, *Fuel*, **173**, 189 (2016).
12. S. V. Lysenko, A. B. Kulikov, M. I. Onishchenko, E. V. Rakhmanov and E. A. Karakhanov, *Moscow Univ. Chem. Bull. (Engl. Transl.)*, **71**(1), 37 (2016).
13. T.-T. Bao, B. Zhou, J. Deng and Z.-J Wu, *J. Shanghai Jiaotong University (Science)*, **19**(6), 721 (2014).
14. J. G. Speight, *Hydrogen in Refineries Hydrogen Science and Engineering: Materials, Processes, Systems and Technology (Book Chapter)*, CRC Press (2016).
15. L. C. Castañeda, A. D. Muñoz and J. Ancheyta, *Catal. Today*, 220-222, **248** (2014).
16. R. Long, K. Picioccio and A. Zagoria, *Petroleum Technology Quarterly*, **16**(3) (2011).
17. F. E. Cruz and Jr. S. De Oliveira, *Int. J. Thermodyn.*, **11**(4), 187 (2008).
18. J. Docekal, *Int. J. Hydrogen Energy*, **11**(11), 709 (1986).
19. L. C. Castañeda, J. A. D. Muñoz and J. Ancheyta, *Fuel*, **90**(12), 3593 (2011).
20. X. Jie, S. Gonzalez-Cortes, T. Xiao, J. Wang, B. Yao, D. R. Slocombe, H. A. Al-Megren, J. R. Dilworth, J. M. Thomas and P. P. Edwards, *Angew. Chem., Int. Ed.*, **56**(34), 10170 (2017).
21. L. Wu, X. Liang, L. Kang and Y. Liu, *Chin. J. Chem. Eng.*, **25**(8), 1061 (2017).
22. S. Sadighi, A. Ahmad and M. Rashidzadeh, *Korean J. Chem. Eng.*, **27**(4), 1099 (2010).
23. G. Zahedi, H. Yaqubi and M. Ba-Shammakh, *Appl. Catal., A*, **358**, 1 (2009).
24. R. Hayati, S. Z. Abghari, S. Sadighi and M. Bayat, *Korean J. Chem. Eng.*, **32**(4), 629 (2015).
25. J. J. Verstraete, K. Le Lannic and I. Guibard, *Chem. Eng. Sci.*, **62**(18-20), 5402 (2007).
26. A. Alvarez and J. Ancheyta, *Appl. Catal., A*, **351**(2), 148 (2008).
27. L. Sunggyu, *Encyclopedia of Chemical Processing*, CRC Press (2005).
28. G. A. Olah, *Hydrocarbon Chemistry*, Wiley, New York (2002).
29. S. B. He. *Studies on the catalysts and the coke deposition behavior of the dehydrogenation of long chain paraffins (C_{10}-C_{19})*, Dalian Institute of Chemical Physics, Chinese Academy of Sciences (2009).
30. D. Sanfilippo and I. Miracca, *Catal. Today*, **111**, 133 (2006).
31. R. S. París, M. E. L'Abbatea, L. F. Liotta, V. Montes, J. Barrientos, F. Regali, A. Ahoe, M. Boutonnet and S. Järås, *Catal. Today*, **275**, 141 (2016).
32. R. A. Rakoczy and P. M. Morse, *Hydrocarbon Processing*, **92**(7) (2013).
33. E. Frantsina, N. Belinskaya and N. Popova, *MATEC Web of Conferences*, **85**, 01023 (2016).
34. E. V. Frantsina, E. N. Ivashkina, E. D. Ivanchina and R. V. Romanovskii, *Chem. Eng. J.*, **238**, 224 (2015).
35. N. S. Belinskaya, E. V. Frantsina and E. D. Ivanchina, *Chem. Eng. J.*, **329**, 283 (2017).
36. E. N. Ivashkina, E. V. Frantsina, R. V. Romanovsky, I. M. Dolganov, E. D. Ivanchina and A. V. Kravtsov, *Catalysis in Industry*, **4**(2), 110 (2012).
37. A. V. Kravtsov, E. D. Ivanchina, E. N. Ivashkina, E. V. Frantsina, S. V. Kiseleva and R. V. Romanovskii, *Pet. Chem.*, **53**(4), 267 (2013).
38. N. S. Belinskaya, E. V. Frantsina, E. D. Ivanchina, N. V. Popova and N. E. Belozertseva, *Pet. Coal*, **58**(7), 695 (2016).
39. N. Chang and Z. Gu, *Korean J. Chem. Eng.*, **31**(5), 780 (2014).
40. S. Yoon, W. C. Choi, Y.-K. Park, H. Y. Kim and C. W. Lee, *Korean J. Chem. Eng.*, **27**(1), 62 (2010).